Nuclear Respiratory Factor 1 Promotes The Growth of Liver Hepatocellular Carcinoma Cells Via E2F1 Transcriptional Activation

Dan Wang
Nantong University
Baolan Wan
Nantong University
Xiaojing Zhang
Affiliated Hospital of Nantong University
Pingping Sun
Affiliated Hospital of Nantong University
Shu Lu
Affiliated Hospital of Nantong University
Chenxu Liu
Nantong University
Li Zhu (zhulizhou@ntu.edu.cn)
Nantong University

Research Article

Keywords: hepatocellular carcinoma, prognosis, cell proliferation, gene expression regulation

Posted Date: September 7th, 2021

DOI: https://doi.org/10.21203/rs.3.rs-858236/v1

Abstract

Background Recent studies have shown that functional mitochondria are essential for cancer cells. Nuclear respiratory factor 1 (NRF1) is a transcription factor that activates mitochondrial biogenesis and the expression of the respiratory chain, but little is known about its role and underlying mechanism in liver hepatocellular carcinoma (LIHC).

Methods NRF1 expression was analyzed via public databases and 24 paired LIHC samples. Clinical-pathological information and follow-up data were collected from 165 patients with LIHC or online datasets. Furthermore, cellular proliferation and the cell cycle were analyzed by MTT, Clone-forming assay and flow cytometric analyses. NRF1 target genes were analyzed by Chromatin immunoprecipitation sequencing (ChIP-Seq). PCR and WB analysis was performed to detect the expression of related genes. ChIP and luciferase activity assays were used to identify NRF1 binding sites.

Results Our results showed that NRF1 expression was upregulated in LIHC compared to normal tissues. NRF1 expression was associated with tumour size and poor prognosis in patients. Knockdown of NRF1 repressed cell proliferation, and overexpression of NRF1 accelerated the G_1/S phase transition. Additionally, data from ChIP-seq pointed out that some NRF1 target genes are involved in the cell cycle. Our findings indicated that NRF1 directly binds to the *E2F1* promoter as a transcription factor and regulates its gene expression.

Conclusion Therefore, this study revealed that NRF1 promotes cancer cell growth via the indirect transcriptional activation of E2F1 and is a potential biomarker in LIHC.

Background

Liver cancer is the third leading cause of cancer death worldwide [1]. Most primary liver cancer occurring worldwide is liver hepatocellular carcinoma (LIHC) [2, 3]. The early diagnosis of LIHC is complicated thus far. The overall five-year survival rate is extremely low because greater than 60% of patients are diagnosed in advanced stages [4–6]. Thus, an effective biomarker is urgently needed to estimate prognosis.

Hepatocytes, which are rich in mitochondria, have developed diverse mechanisms to maintain mitochondrial homeostasis by regulating mitochondrial dynamics, biogenesis and degradation [7, 8]. Mitochondrial reactive oxygen species (mROS) mediate metabolic pathway signalling; alterations in these pathways affect the development and progression of chronic liver diseases and tumours [9, 10]. Paradoxically, mitochondrial metabolism can be both advantageous and detrimental to cancer metastasis and therapy resistance [10]. Recently, emerging studies have shown that functional mitochondria are essential for cancer cells [11]. Mitochondria in cancer cells are different from their normal counterparts in structure and function [12–14]. Beyond the classical role in energy and metabolic mechanisms, both mitochondrial DNA (mtDNA) defects and increased mitochondrial fission have been reported in many cancers [15]. Importantly, mitochondrial biogenesis and quality control are often

upregulated in cancers and play a critical role in oncogenic signalling pathways [11, 16]. Nuclear respiratory factor 1 (NRF1) is a transcription factor known to directly regulate several nuclear-encoded electron transport chain proteins [17]. In addition, NRF1 is indirectly involved in regulating the expression of mtDNA transcription by coactivation with peroxisome proliferator-activated receptor gamma coactivator 1α (PGC-1α) [18]. Thus, NRF1 plays an essential role in mitochondrial biogenesis. Satoh *et al* identified that NRF1 target genes played a pivotal role in the regulation of extramitochondrial biological processes, including DNA damage repair, protein translation initiation, and ubiquitin-mediated protein degradation [19]. NRF1 has also been identified as a valuable biomarker for breast cancer diagnosis and prognosis [20].

However, NRF1 and its target genes, whose expression pattern and biological function in tumours, are largely unknown. In this study, we aimed to investigate whether NRF1 can affect liver cancer cell growth. These findings might uncover a mechanism by which NRF1 is involved in LIHC progression.

Materials And Methods

Study populations

A total of 165 formalin-fixed, paraffin-embedded samples were excised from fresh LIHC surgical samples. The clinicopathological features included sex, age at diagnosis, differentiation, vascular invasion, TNM stage, tumour size and cirrhosis. None of the patients received radiotherapy, chemotherapy, or immunotherapy prior to surgery. The overall survival duration was defined as the interval from the date of first biopsy to the date of death from disease.

Immunohistochemistry (IHC)

LIHC tissue microarray (TMA) slides from patients were used for NRF1 staining with a Tissue Microarray System (Quick-Ray, UT06, UNITMA, Korea). Core tissue biopsies (2 mm in diameter), which were taken from individual paraffin-embedded sample sections, were arranged in new recipient paraffin blocks. IHC analysis was performed as previously described [21]. The slides were incubated with the primary antibody against NRF1 (Abcam, Cambridge, MA, USA) at 4 °C overnight. Three trained pathologists were blinded to evaluate NRF1 immunostaining. There were two estimated variables: intensity (0 to 3 as negative, weak, moderate or strong) and percentage (0% to 100%). The degree of NRF1 expression was quantified using a two-level grading system defined as follows: score $\leq$ 60 defined as low, otherwise defined as high.

Tumour Immune Estimation Resource (TIMER) and Gene Expression Profiling Interactive Analysis (GEPIA) Database Analysis

The level of NRF1 mRNA expression in different tumour types was obtained from TIMER2.0 (http://timer.cistrome.org/) [22, 23]. GEPIA2 (http://gepia2.cancer-pku.cn/#index) was employed to profile

the expression of NRF1 in different cancer stages and generate disease-free survival curves based on the expression status of NRF1 [24].

Cell culture, cell transfection and lentivirus infection

HepG2 cells were maintained in Dulbecco's modified Eagle's medium (DMEM) (HyClone, UT, USA) containing 10% foetal bovine serum (HyClone, UT, USA) and were cultured at 37 °C with 5% CO_2 in an incubator. Cells were transiently transfected with plasmids or siRNA duplexes using Lipofectamine 2000 Transfection Reagent (Invitrogen, CA, USA) following the manufacturer's protocol. NRF1 overexpression constructs were generated into the Ubi-MCS-3FLAG-CBh-gcGFP-IRES-puromycin lentiviral vector (GeneChem, Shanghai, CHN). The lentivirus infection was manipulated according to the instructions.

Chromatin immunoprecipitation sequencing (ChIP-Seq) dataset of NRF1 binding sites and molecular pathway analysis

ChIP was performed using the SimpleChIP® Plus Enzymatic Chromatin IP Kit (Cell Signaling Technology, MA, USA) as described in the manufacturer's protocol. Briefly, cells were washed and fixed in 1% formaldehyde at room temperature. Then, the cells were collected and lysed to release the nuclei. Nuclei were then isolated before being subjected to micrococcal nuclease. The lysate was then immunoprecipitated with NRF1 antibodies (Abcam, MA, USA) or a negative control IgG. The pulled-down chromatin was washed, reverse-crosslinked, purified and detected by deep sequencing (Vazyme Biotech, Nanjing, China). To identify the pathways relevant to ChIP-Seq-based NRF1 target genes, we used Database for Annotation, Visualization and Integrated Discovery (DAVID) v6.8 (https://david.abcc.ncifcrf.gov/) to analyse the sequencing data.

Gene Silencing

Human NRF1-specific siRNA (siNRF1) duplexes were designed and synthesized by GenePharma Co., Ltd. (GenePharma, Shanghai, CHN). The siNRF1 sequences were as follows: siNRF1, 5'-CACAUUGGCUGAUGCUUCAUU-3'.

RNA Isolation and Quantitative Real-time PCR

RNA was isolated using TRIzol reagent (Invitrogen, CA, USA) and treated with DNase I (Promega, WI, USA) before cDNA synthesis. cDNA was synthesized by a Transcript First-Strand cDNA Synthesis Kit (Vazyme Biotech, Nanjing, China). Quantitative real-time PCR was performed using AceQ qPCR SYBR Green Master Mix (High ROX Premixed) (Vazyme, Nanjing, CHN) in a StepOne Plus Real-time PCR System (Applied Biosystems, Singapore city, Singapore). The primer sequences were as follows: *E2F1*, F: 5'-CATCCCAGGAGGTCACTTCTG-3' and R: 5'-GACAACAGCGGTTCTTGCTC-3'; *ACTB*, F: 5'-CATGTACGTTGCTATCCAGGC-3' and R: 5'- CTCCTTAATGTCACGCACGAT-3'; *CCNE1*: F: 5'-ACTCAACGTGCAAGCCTCG-3' and R: 5'-GCTCAAGAAAGTGCTGATCCC-3'; *CDK2*, F: 5'-

CCAGGAGTTACTTCTATGCCTGA-3’ and R: 5’-TTCATCCAGGGGAGGTACAAC-3’. Melting curves were generated to confirm primer specificity.

Western Blot

Cells were collected and lysed with cell lysis buffer (Beyotime, Shanghai, China). Whole-cell extracts were resolved by 10% SDS–PAGE and electrophoretically transferred to polyvinylidene difluoride membranes (Roche Diagnostics, Mannheim, Germany). The membranes were blocked and then incubated with anti-NRF1, anti-β-actin or anti-E2F1 antibodies (Abcam, Cambridge, MA, USA) at 4 °C overnight, followed by incubation with the appropriate horseradish peroxidase-conjugated secondary antibodies (Jackson ImmunoResearch, PA, USA). The chemiluminescence reaction was performed using ECL reagent (Thermo Scientific, IL, USA).

Clone-forming assay

The cells were seeded (10^3 cells/well) onto 12-well plates and cultured for 3 days. The cells were fixed with 4% paraformaldehyde for 30 min and stained with crystal violet (Sigma–Aldrich, MO, USA). The cell clones were photographed and counted. Each experimental group was performed in triplicate.

Cell proliferation assay

The cells were seeded onto 96-well plates at a density of 2×10^3 cells/well and cultured for 96 h. Then, 100 μL of 3-(4,5-dimethylthiazol-2-yl)-2,5-diphenyl-tetrazolium bromide (MTT; Sigma–Aldrich, MO, USA; 5 mg/mL) in PBS was added to each 96-well plate, and the cells were incubated for an additional 4 h. Then, the supernatants were removed and replaced with 100 μL dimethyl sulfoxide to dissolve the formazan crystals. Optical density (OD) was measured at 570 nm wavelength by an ELX-800 Microplate assay reader (Bio-tek, USA). The OD_{570} values indicated changes in cell proliferation.

Cell cycle analysis

Cells were treated with serum-free medium for synchronization. To assess the cell cycle distribution, all the above cells were collected and fixed in 70% ethanol overnight. After removal of the ethanol, samples were washed three times with PBS and then incubated with RNase A at 4 °C for 30 min. Next, samples were stained with propidium iodide (50 μg/ml) and evaluated by a Gallios flow cytometer (Beckman). The subsequent analysis was conducted by MultiCycle software.

Chromatin immunoprecipitation

Cells were fixed with formaldehyde, and sonicated nuclear lysates were processed for immunoprecipitation with NRF1 antibody or normal IgG (Abcam, Cambridge, MA, USA). ChIP DNA fragments were processed for quantitative real-time PCR. The amount of amplified DNA was roughly comparable to that obtained using approximately 2% of the total input chromatin as templates. Primers were designed with *E2F1* promoter binding sites: primer 1 (-333/-17), F: 5’-AGAAAGGTCAGTGGGATGCG-3’

and R: 5′-CCAAATCCTTTTTGCCGCGA-3′, which was amplified region of 317-bp; primer 2 (-1291/-869), F: 5′-AGCCTCTGTTTCTTTCATAACCT-3′ and R: 5′-TCGAGACCAGCCTGATCAACA-3′, which was amplified region of 422-bp.

Plasmid Constructs

Genomic DNA was used as the template to construct *E2F1* promoter reporter plasmids. Different truncations of the human *E2F1* promoter were cloned into the pGL3-Basic vector (Promega, WI, USA). Primer sequences for *E2F1* (-333/-17) are F: 5′-GCTAGCAGAAAGGTCAGTGGGATGCG-3′ (NheI site is underlined) and R: 5′-AAGCTTCCAAATCCTTTTTGCCGCGA -3′ (HindIII site is underlined); *E2F1* (-1291/-869) primer sequences are F: 5′-GCTAGCAGCCTCTGTTTCTTTCATAACCT-3′ (NheI site is underlined) and R: 5′-AAGCTTAGCCTCTGTTTCTTTCATAACCT-3′ (HindIII site is underlined) The NRF1 binding sites in *E2F1* promoter were mutated, respectively. Site-directed mutagenesis of putative NRF1 binding sites was generated using a QuikChange site-directed mutagenesis kit (Stratagene, CA, USA). The expression plasmids for wild-type NRF1 and DN NRF1 (a dominant-negative form) were constructed according to a method described previously [25, 26]. All constructs were verified by sequencing.

Dual-luciferase Reporter Assays

Each well of cells was transiently cotransfected with *E2F1* promoter luciferase constructs and pRL-TK (Promega, WI, USA) as an internal control. Cells were lysed and collected to detect luciferase activity by the Dual-Luciferase Reporter Assay System (Promega, WI, USA). The firefly/*Renilla* luciferase activity measurements were recorded according to the manufacturer's protocol.

Statistical Analysis

The differences in NRF1 expression in tumour and adjacent tissue were assessed using paired t tests. Correlations between clinicopathologic features and NRF1 expression were evaluated by the chi-square test. Multivariate survival analysis was performed with Cox regression. Statistical significance was determined by one-way ANOVA, followed by the post hoc Tukey multiple comparison test or two-way ANOVA, followed by Bonferroni's multiple comparisons test. All *P* values reported are from two-sided tests, and the threshold for significance was set at $P = 0.05$. The statistical analyses were performed using STATA version 13.0 (StataCorp, TX, USA).

Results

The difference in NRF1 expression in LIHC and normal tissues

The TIMER database showed that NRF1 mRNA expression was significantly higher in CHOL (bladder urothelial carcinoma), COAD (colon adenocarcinoma), KIRC (kidney renal clear cell carcinoma), KIRP (kidney renal papillary cell carcinoma), and LIHC (liver hepatocellular carcinoma), while it was lower in BRCA (breast invasive carcinoma), LUAD (lung adenocarcinoma), UCEC (uterine corpus endometrial

carcinoma), PRAD (prostate adenocarcinoma) and THCA (thyroid carcinoma) than in normal tissues (Fig. 1a). The NRF1 expression in LIHC from GEPIA2 datasets was consistent with TIMER (Fig. 1b).

Since the TCGA database contains mRNA expression data, we used IHC to validate *in situ* protein expression in patient samples. Representative images of NRF1 staining are shown in Figure. 1c. Positive NRF1 staining was predominantly localized to the nucleus. NRF1 was negative or weakly stained in normal tissues. Moderate or strong NRF1 staining was found in LIHC. Next, we examined NRF1 protein expression in 24 pairs of LIHC and adjacent noncancerous tissues. The NRF1 expression levels were significantly higher in tumour tissues than in nontumour tissues (Fig. 1d & e).

NRF1 expression correlated with clinicopathological parameters and poor prognosis

The distribution of LIHC patients is shown in Table 1. From our data, NRF1 expression presented a correlation with vascular invasion ($P = 0.015$), TNM stage ($P = 0.004$) and tumour size ($P = 0.004$). In contrast, no correlation ($P > 0.05$) was observed between NRF1 expression and other clinical parameters, including age at diagnosis, differentiation and cirrhosis (Table 2). GEPIA2 datasets were also utilized to analyse the association of NRF1 expression and clinicopathological parameters. As shown in Fig. 2a, there were significant differences between different stages in LIHC patients ($P < 0.01$). Kaplan–Meier survival curves revealed that LIHC patients with high NRF1 expression had significantly poorer disease-free survival (DFS) ($P < 0.01$, HR (hazard ratio) = 1.5, Fig. 2b). The results of Cox regression showed that cirrhosis ($P = 0.018$) and NRF1 expression ($P = 0.004$) correlated with survival of LIHC, and TNM stage showed a strong tendency towards statistical significance ($P = 0.052$). The relation remained significant after adjustment, and NRF1 ($P = 0.013$; $HR_{adj} = 1.87$; 95% CI = 1.14–3.06) was found to be an independent prognostic factor (Table 3).

Table 1
Characteristics of the populations studied

characteristic	detail
N	165
Age	52.64 ± 10.11 years (range 31–79 years)[†]
Sex	125 male, 40 female
Follow-up	44.59 ± 28.96 months (range 1–111 months)[†]

[†]mean ± SD; range in parentheses.

Table 2
NRF1 expression and clinical variables in liver hepatocellular carcinoma

	NRF1		*p*
	Low	High	
Total	**89 (53.94%)**	**76 (46.06%)**	
Gender			0.212
female	25 (62.50%)	15 (37.50%)	
male	64 (51.20%)	61 (48.80%)	
Age			0.804
≤ 50	51 (53.13%)	45 (46.87%)	
> 50	38 (55.07%)	31 (44.93%)	
Grade			0.268
well & moderate	72 (56.25%)	56 (43.75%)	
poor	17 (45.95%)	20 (54.05%)	
Vascular invasion			0.015*
no	60 (61.86%)	37 (38.14%)	
yes	29 (42.65%)	39 (57.35%)	
TNM			0.004**
	41 (64.06%)	23 (35.94%)	
	38 (56.72%)	29 (43.28%)	
	10 (29.41%)	24 (70.59%)	
Tumor size			0.004**
≤ 5 cm	62 (63.27%)	36 (36.73%)	
> 5 cm	27 (40.30%)	40 (59.70%)	
Cirrhosis			0.224
no	35 (60.34%)	23 (39.66%)	
yes	54 (50.47%)	53 (49.53%)	
*$p < 0.05$, **$p < 0.01$			

Table 3
Cox regression analysis of prognostic factors for 5-year survival in hepatocellular carcinoma

	Univariate analysis			Multivariate analysis		
	p	HR	95% CI	*p*	HR	95% CI
Gender	0.742	0.91	0.53–1.58			
male *vs* female						
Age	0.227	0.73	0.43–1.22			
< 55 *vs* ≥ 55						
Grade	0.801	1.08	0.61 – 1.91			
well & moderate *vs* poor						
Vessel invasion	0.208	1.36	0.84–2.21			
no *vs* yes						
TNM	0.052	1.40	1.00–1.97			
□ *vs* □ & □						
Tumor size	0.071	1.56	0.96–2.51			
≤ 5 cm *vs* > 5 cm						
Cirrhosis	0.018*	1.98	1.13–3.47	0.057	1.74	0.98–3.09
no *vs* yes						
NRF1	0.004**	2.05	1.26–3.34	0.013*	1.87	1.14–3.06
low *vs* high						
*$p < 0.05$, **$p < 0.01$						

Effect of NRF1 on cell proliferation

Since NRF1 was significantly associated with tumour size, we investigated whether NRF1 expression correlated with liver cancer cell growth. The clone formation assay showed that the siNRF1 group had fewer clones than the siCtrl group (Fig. 3a – 3c). MTT results revealed that fewer cells were found in the siNRF1 group than in the siCtrl group (Fig. 3d). Next, we analysed the proportion of cell populations in each cell cycle phase. We used serum starvation-induced cell cycle synchronization to accumulate the cell population prior to G_0/G_1. After refeeding with FBS for 24 h, a mass of cells was stimulated to enter the cell cycle and started mitosis simultaneously. The results showed that NRF1 overexpression resulted

in a reduction in cells in the G_0/G_1 phase and accumulation in the S phase compared with the control, suggesting that NRF1 was involved in the G_1/S transition (Fig. 3e).

NRF1 induced E2F1 mRNA expression

ChIP-Seq was performed to detect whether NRF1 target genes were involved in cell growth. All 3984 stringent ChIP-Seq peaks were identified on the Illumina HiSeq analysis platform. DAVID was used to identify 192 NRF1 target genes that showed a correlation with the cell cycle, including G_1/S phase transition genes (Tables S1–S2). The Rb/E2F network has a critical role in regulating cell cycle progression and cell fate decisions [27]. Then, the role of NRF1 in regulating E2F1 expression was examined.

As evident from Figure. 4a, there was a striking reduction in E2F1 mRNA in siNRF1-transfected cells. Then, we verified that the NRF1 WT construct resulted in a marked increase in E2F1 mRNA compared with the pcDNA3.1 control (Fig. 4b). Cyclin E1 (CCNE1), which is a target of E2F1, is the limiting factor for G_1 phase progression and S phase entry [28, 29]. Cyclin E1 activates cyclin-dependent protein kinase 2 (CDK2) shortly before entry of cells into the S phase [30]. Given that cyclin E1 and CDK2 are important regulators of the G_1/S transition, we questioned whether there was a difference in CCNE1 and CDK2 expression. Consistent with the E2F1 downregulation, attenuation of CCNE1 and CDK2 expression resulted in siNRF1-transfected cells compared with controls (Fig. 4a). In line with our expectations, we observed that CCNE1 and CDK2 were upregulated in the NRF1-overexpressing group (Fig. 4b).

Identification of NRF1 binding sites in the promoter of the human E2F1 gene

To identify putative binding sites of NRF1 in the promoter proximal regions of *E2F1*, we performed an *in silico* search using the open-access database JASPAR (Table S3). As shown in Fig. 5a, the analysis identified five putative NRF1 binding sites. The *in vivo* binding of NRF1 to the human *E2F1* promoter was tested by ChIP analysis. Compared with IgG control samples, immunoprecipitated *E2F1* promoter fragments (from − 331 to -17 and − 1291 to -869) were significantly enriched using a specific NRF1 antibody (Figure. 5b & 5c).

We used a luciferase reporter plasmid driven by the human E2F1 promoter region to further evaluate the role of NRF1 in E2F1 transcription. The luciferase activities of the *E2F1* (-331/-17) and (-1291/-869) constructs were significantly higher than that of the pGL3-Basic construct. Compared with the pcDNA3.1-transfected group, the luciferase activities of *E2F1* promoter constructs were markedly increased in pcDNA3-NRF1-transfected cells. Additionally, no significant changes in E2F1 promoter constructs were detected in the NRF1 DN group (Fig. 5d).

Furthermore, different mutations were detected to identify which nucleotides were essential for *E2F1* transcription by NRF1 (Fig. 5e). Exogenous NRF1 overexpression had no effect on the luciferase activity of *E2F1* (-333/-17 mut1 ~ 3) and *E2F1* (-1291/-869 mut2). However, a consequent increase in luciferase activity was observed when cells were cotransfected with pcDNA3-NRF1 and E2F1 (-1291/-869 mut1).

These results illustrated that four functional NRF1 binding sites (from − 205 to -193, -163 to -153, -199 to -189 and − 1262 to -1252) were essential for *E2F1* transcription activity (Fig. 5f).

Discussion

It has been identified that the biology of mitochondria in cancer is important to our understanding of cancer biology, as many classical cancer hallmarks result in altered mitochondrial function[10, 11, 31]. Significant efforts have been made to characterize the extramitochondrial biological processes of NRF1[25, 26, 32]. NRF1 may orchestrate both MYC and E2F4 to regulate common target genes linked to multiple networks in the development and progression of cancer [33]. It has been suggested that NRF1 is essential for lysine-specific demethylase 1 (LSD1) histone modification. The complex of NRF1, LSD1 and oestrogen-receptor related α (ERRα) is required for cell invasion in a matrix metalloprotease 1 (MMP1)-dependent manner [34]. NRF1 also forms an activator complex with egl-9 family hypoxia inducible factor 2 (EglN2) to promote ferridoxin reductase (FDXR) transcription activation. FDXR regulates mitochondrial function and contributes to breast tumorigenesis *in vitro* and *in vivo* [35]. Thus, NRF1 inevitably needs to be taken into account when evaluating prognostics and therapeutic options for cancer patients.

Mitochondria are of great importance to physiology [36]. For decades, mitochondria are symmetrically partitioned to daughter cells during typical cell division [37]. Lung cancer cell lines exhibit an imbalance of mitofusin-2 (Mfn-2) and dynamin-related protein (Drp-1) expression, which mediates mitochondrial fusion and fission [38]. Drp1 and Mfn-2 play a crucial role in controlling cell cycle-associated changes in mitochondrial morphology [39–41]. An essential step in mitochondrial biogenesis is mitochondrial fission [42]. The repression of mitochondrial fission and/or promotion of mitochondrial fusion promotes mitochondrial biogenesis [43]. NRF1 is a key component of the regulatory network that controls mitochondrial biogenesis. We guessed that NRF1 involved in cell cycle. In our study, we demonstrated that NRF1 was correlated with some clinical variables (TNM stage, tumour size and vascular invasion) in LIHC. NRF1 was associated with poor disease-free survival and functioned independently as a prognostic factor for LIHC patients. Based on our data, NRF1 is involved in tumour growth. Additionally, ChIP-Seq identified some NRF1 target genes that participate in the cell cycle, especially in the G_1/S phase transition. Mitra *et al* demonstrated a relationship between the mitochondrial form and cell cycle control at the G_1/S phase [44].

E2F1 regulates the expression of a number of genes involved in progression through G_1 and into the S-phase of the cell cycle [45]. Beyond that, E2F1 was associated with enhanced tumour cell apoptosis or proliferation depending on cell lines and mouse models [46]. E2F1 has contradictory roles in cancer, and its function has been under debate for years [47, 48]. Although the mechanisms have generated some controversy, the core regulatory network of E2F1/Rb that controls the cell cycle in the G_1/S transition is generally accepted [49]. Previous findings revealed that NRF1 binds to the E2F6 gene promoter [50]. Cam *et al* predicted the existence of NRF1 binding sites in E2F target promoters by motif-finding algorithms [51]. Here, we demonstrated that there were four NRF1 binding sites on the *E2F1* promoter that

maintained positive transcription. Our results confirmed their predictions and suggested that there is an existing link between NRF1 and cell replication.

Several limitations could influence the outcomes of this study. First, our study was retrospective and had a relatively small sample size. DFS analysis is based on RNA-seq data retrieved from public repositories. Hence, the quality and quantity of data can influence the study outcomes, although we verified some outcomes by testing our own clinical samples. Second, racial or ethnic differences were not explained or discussed in our study.

Conclusions

This study indicated that NRF1 is involved in cancer growth by regulating *E2F1* transcription. NRF1 is also a valuable prognostic biomarker for LIHC.

Abbreviations

NRF1: nuclear respiratory factor 1

LIHC: hepatocellular carcinoma

mtDNA: mitochondrial DNA

PGC-1α: peroxisome proliferator-activated receptor gamma coactivator 1α

TCGA: The Cancer Genome Atlas

TIMER: Tumor Immune Estimation Resource

GEPIA: Gene Expression Profiling Interactive Analysis

CHOL: bladder urothelial carcinoma

COAD: colon adenocarcinoma

KIRC: kidney renal clear cell carcinoma

KIRP: kidney renal papillary cell carcinoma

LIHC: liver hepatocellular carcinoma

BRCA: breast invasive carcinoma

LUAD: lung Adenocarcinoma

UCEC: uterine corpus endometrial carcinoma

PRAD: prostate adenocarcinoma

THCA: thyroid carcinoma

siRNA: small interfering RNA

HR: hazard ratio

GO: gene ontology

DFS: disease-free survival

IHC: immunohistochemistry

CCNE1: cyclin E1

CDK2: cyclin-dependent protein kinase 2

RT–PCR: reverse transcriptase-polymerase chain reaction

ChIP: chromatin immunoprecipitation

LSD1: lysine-specific demethylase 1

ERRα: estrogen-receptor related α

EglN2: egl-9 family hypoxia inducible factor 2

FDXR: promote ferridoxin reductase

Mfn-2: mitofusin-2

Drp-1: dynamin-related protein

Declarations

Ethics approval and consent to participate: All procedures were performed in accordance with the Declaration of Helsinki and complied with relevant guidelines and regulations. The study was approved by the Ethics Committee of the Human Research Ethics Committee of the Affiliated Hospital of Nantong University (2017-K036). Written informed consent was obtained from the patients for publication of this study.

Consent for publication Not applicable.

Availability of data and materials: The datasets used and/or analyzed during the current study are available from the corresponding author on reasonable request.

Competing interests: The authors declare that they have no competing interests.

Fundings: This research was funded by National Natural Science Foundation of China (Grant Nos. 81702874 & 31471141), National College Students' innovation and entrepreneurship training program (202110304032Z), Nantong Commission of Health (No. MB2020081) and Special Foundation for Excellent Young Teachers and Principals Program of Jiangsu Province (2020).

Author Contributions: Conceptualization, LZ and DW. Data curation: DW, BLW, XJZ and PPS. Formal analysis: DW, BLW and SL. Funding acquisition: LZ, DW, SL and CXL. Investigation: DW. Methodology: DW, BLW, XJZ and CXL. Resources: LZ. Software: DW. Supervision: LZ. Validation: DW, BLW, XJZ, PPS and LZ. Writing (original draft): DW. Writing (review & editing): LZ.

References

1. Sung, H., J. Ferlay, R.L. Siegel, M. Laversanne, I. Soerjomataram, A. Jemal, et al., Global Cancer Statistics 2020: GLOBOCAN Estimates of Incidence and Mortality Worldwide for 36 Cancers in 185 Countries. CA Cancer J Clin, 2021. 71(3): p. 209–249.
2. Sia, D., A. Villanueva, S.L. Friedman, and J.M. Llovet, Liver Cancer Cell of Origin, Molecular Class, and Effects on Patient Prognosis. Gastroenterology, 2017. 152(4): p. 745–761.
3. Forner, A., M. Reig, and J. Bruix, Hepatocellular carcinoma. Lancet, 2018. 391(10127): p. 1301–1314.
4. Tsuchiya, N., Y. Sawada, I. Endo, K. Saito, Y. Uemura, and T. Nakatsura, Biomarkers for the early diagnosis of hepatocellular carcinoma. World J Gastroenterol, 2015. 21(37): p. 10573–10583.
5. Keating, G.M., Sorafenib: A Review in Hepatocellular Carcinoma. Target Oncol, 2017. 12(2): p. 243–253.
6. Xing, M., X. Wang, R.A. Kiken, L. He, and J.-Y. Zhang, Immunodiagnostic Biomarkers for Hepatocellular Carcinoma (HCC): The First Step in Detection and Treatment. International Journal of Molecular Sciences, 2021. 22(11): p. 6139.
7. Grattagliano, I., O. de Bari, T.C. Bernardo, P.J. Oliveira, D.Q. Wang, and P. Portincasa, Role of mitochondria in nonalcoholic fatty liver disease–from origin to propagation. Clin Biochem, 2012. 45(9): p. 610–618.
8. Kang, J.W., J.M. Hong, and S.M. Lee, Melatonin enhances mitophagy and mitochondrial biogenesis in rats with carbon tetrachloride-induced liver fibrosis. J Pineal Res, 2016. 60(4): p. 383–393.
9. Mansouri, A., C.H. Gattolliat, and T. Asselah, Mitochondrial Dysfunction and Signaling in Chronic Liver Diseases. Gastroenterology, 2018. 155(3): p. 629–647.
10. Valcarcel-Jimenez, L., E. Gaude, V. Torrano, C. Frezza, and A. Carracedo, Mitochondrial Metabolism: Yin and Yang for Tumor Progression. Trends Endocrinol Metab, 2017. 28(10): p. 748–757.
11. Vyas, S., E. Zaganjor, and M.C. Haigis, Mitochondria and Cancer. Cell, 2016. 166(3): p. 555–566.
12. Gogvadze, V., S. Orrenius, and B. Zhivotovsky, Mitochondria in cancer cells: what is so special about them? Trends Cell Biol, 2008. 18(4): p. 165–173.

13. Weinberg, S.E. and N.S. Chandel, Targeting mitochondria metabolism for cancer therapy. Nature Chemical Biology, 2015. 11(1): p. 9–15.
14. Ksiezakowska-Lakoma, K., M. Zyla, and J.R. Wilczynski, Mitochondrial dysfunction in cancer. Prz Menopauzalny, 2014. 13(2): p. 136–144.
15. Srinivasan, S., M. Guha, A. Kashina, and N.G. Avadhani, Mitochondrial dysfunction and mitochondrial dynamics-The cancer connection. Biochim Biophys Acta Bioenerg, 2017. 1858(8): p. 602–614.
16. Zong, W.X., J.D. Rabinowitz, and E. White, Mitochondria and Cancer. Mol Cell, 2016. 61(5): p. 667–676.
17. Scarpulla, R.C., Transcriptional paradigms in mammalian mitochondrial biogenesis and function. Physiological Reviews, 2008. 88(2): p. 611–638.
18. Scarpulla, R.C., Nuclear activators and coactivators in mammalian mitochondrial biogenesis. Biochim Biophys Acta, 2002. 1576(1–2): p. 1–14.
19. Satoh, J.-I., N. Kawana, and Y. Yamamoto, Pathway Analysis of ChIP-Seq-Based NRF1 Target Genes Suggests a Logical Hypothesis of their Involvement in the Pathogenesis of Neurodegenerative Diseases. Gene regulation and systems biology, 2013. 7: p. 139–152.
20. Ramos, J., J. Das, Q. Felty, C. Yoo, R. Poppiti, D. Murrell, et al., NRF1 motif sequence-enriched genes involved in ER/PR -ve HER2 + ve breast cancer signaling pathways. Breast Cancer Res Treat, 2018. 172(2): p. 469–485.
21. Sun, R., X. Wang, H. Zhu, H. Mei, W. Wang, S. Zhang, et al., Prognostic value of LAMP3 and TP53 overexpression in benign and malignant gastrointestinal tissues. Oncotarget, 2014. 5(23): p. 12398–12409.
22. Li, T., J. Fan, B. Wang, N. Traugh, Q. Chen, J.S. Liu, et al., TIMER: A Web Server for Comprehensive Analysis of Tumor-Infiltrating Immune Cells. Cancer Res, 2017. 77(21): p. e108-e110.
23. Li, B., E. Severson, J.C. Pignon, H. Zhao, T. Li, J. Novak, et al., Comprehensive analyses of tumor immunity: implications for cancer immunotherapy. Genome Biol, 2016. 17(1): p. 174.
24. Tang, Z., C. Li, B. Kang, G. Gao, and Z. Zhang, GEPIA: a web server for cancer and normal gene expression profiling and interactive analyses. Nucleic Acids Res, 2017. 45(W1): p. W98-W102.
25. Solecki, D., G. Bernhardt, M. Lipp, and E. Wimmer, Identification of a nuclear respiratory factor-1 binding site within the core promoter of the human polio virus receptor/CD155 gene. The Journal of biological chemistry, 2000. 275(17): p. 12453–12462.
26. Wang, D., J. Zhang, Y. Lu, Q. Luo, and L. Zhu, Nuclear respiratory factor-1 (NRF-1) regulated hypoxia-inducible factor-1alpha (HIF-1alpha) under hypoxia in HEK293T. IUBMB Life, 2016. 68(9): p. 748–755.
27. Shats, I., M. Deng, A. Davidovich, C. Zhang, J.S. Kwon, D. Manandhar, et al., Expression level is a key determinant of E2F1-mediated cell fate. Cell Death Differ, 2017. 24(4): p. 626–637.

28. Richardson, H., L.V. O'Keefe, T. Marty, and R. Saint, Ectopic cyclin E expression induces premature entry into S phase and disrupts pattern formation in the Drosophila eye imaginal disc. Development, 1995. 121(10): p. 3371–3379.
29. Ohtani, K., J. DeGregori, and J.R. Nevins, Regulation of the cyclin E gene by transcription factor E2F1. Proc Natl Acad Sci U S A, 1995. 92(26): p. 12146–12150.
30. Honda, R., E.D. Lowe, E. Dubinina, V. Skamnaki, A. Cook, N.R. Brown, et al., The structure of cyclin E1/CDK2: implications for CDK2 activation and CDK2-independent roles. EMBO J, 2005. 24(3): p. 452–463.
31. Porporato, P.E., N. Filigheddu, J.M.B. Pedro, G. Kroemer, and L. Galluzzi, Mitochondrial metabolism and cancer. Cell Res, 2018. 28(3): p. 265–280.
32. Johar, K., A. Priya, and M.T.T. Wong-Riley, Regulation of Na+/K+-ATPase by Nuclear Respiratory Factor 1 IMPLICATION IN THE TIGHT COUPLING OF NEURONAL ACTIVITY, ENERGY GENERATION, AND ENERGY CONSUMPTION. Journal of Biological Chemistry, 2012. 287(48): p. 40381–40390.
33. Bhawe, K. and D. Roy, Interplay between NRF1, E2F4 and MYC transcription factors regulating common target genes contributes to cancer development and progression. Cellular Oncology (Dordrecht), 2018. 41(5): p. 465–484.
34. Zhang, L., J. Carnesecchi, C. Cerutti, V. Tribollet, S. Perian, C. Forcet, et al., LSD1-ERRalpha complex requires NRF1 to positively regulate transcription and cell invasion. Sci Rep, 2018. 8(1): p. 10041.
35. Zhang, J., C. Wang, X. Chen, M. Takada, C. Fan, X. Zheng, et al., EglN2 associates with the NRF1-PGC1alpha complex and controls mitochondrial function in breast cancer. EMBO J, 2015. 34(23): p. 2953–2970.
36. Chen, H. and D.C. Chan, Mitochondrial Dynamics in Regulating the Unique Phenotypes of Cancer and Stem Cells. Cell Metabolism, 2017. 26(1): p. 39–48.
37. Christiansen, E.G., Orientation of the mitochondria during mitosis. Nature, 1949. 163(4140): p. 361.
38. Rehman, J., H.J. Zhang, P.T. Toth, Y. Zhang, G. Marsboom, Z. Hong, et al., Inhibition of mitochondrial fission prevents cell cycle progression in lung cancer. FASEB J, 2012. 26(5): p. 2175–2186.
39. Chen, H. and D.C. Chan, Mitochondrial Dynamics in Regulating the Unique Phenotypes of Cancer and Stem Cells. Cell Metab, 2017. 26(1): p. 39–48.
40. Rehman, J., H.J. Zhang, P.T. Toth, Y. Zhang, G. Marsboom, Z. Hong, et al., Inhibition of mitochondrial fission prevents cell cycle progression in lung cancer. The FASEB Journal, 2012. 26(5): p. 2175–2186.
41. Kashatus, D.F., K.-H. Lim, D.C. Brady, N.L.K. Pershing, A.D. Cox, and C.M. Counter, RALA and RALBP1 regulate mitochondrial fission at mitosis. Nature Cell Biology, 2011. 13(9): p. 1108–1115.
42. Berman, S.B., F.J. Pineda, and J.M. Hardwick, Mitochondrial fission and fusion dynamics: the long and short of it. Cell Death Differ, 2008. 15(7): p. 1147–1152.
43. Peng, K., L. Yang, J. Wang, F. Ye, G. Dan, Y. Zhao, et al., The Interaction of Mitochondrial Biogenesis and Fission/Fusion Mediated by PGC-1alpha Regulates Rotenone-Induced Dopaminergic

Neurotoxicity. Mol Neurobiol, 2017. 54(5): p. 3783–3797.

44. Mitra, K., C. Wunder, B. Roysam, G. Lin, and J. Lippincott-Schwartz, A hyperfused mitochondrial state achieved at G1-S regulates cyclin E buildup and entry into S phase. Proc Natl Acad Sci U S A, 2009. 106(29): p. 11960–11965.
45. Johnson, D.G. and R. Schneider-Broussard, Role of E2F in cell cycle control and cancer. Front Biosci, 1998. 3: p. d447-448.
46. Meng, P. and R. Ghosh, Transcription addiction: can we garner the Yin and Yang functions of E2F1 for cancer therapy? Cell Death & Disease, 2014. 5.
47. Wong, J.V., P. Dong, J.R. Nevins, B. Mathey-Prevot, and L. You, Network calisthenics: control of E2F dynamics in cell cycle entry. Cell cycle (Georgetown, Tex.), 2011. 10(18): p. 3086–3094.
48. Engelmann, D. and B.M. Putzer, The Dark Side of E2F1: In Transit beyond Apoptosis. Cancer Research, 2012. 72(3): p. 571–575.
49. van den Heuvel, S. and N.J. Dyson, Conserved functions of the pRB and E2F families. Nature Reviews Molecular Cell Biology, 2008. 9(9): p. 713–724.
50. Kherrouche, Z., Y. De Launoit, and D. Monte, The NRF-1/alpha-PAL transcription factor regulates human E2F6 promoter activity. Biochemical Journal, 2004. 383: p. 529–536.
51. Cam, H., E. Balciunaite, A. Blais, A. Spektor, R.C. Scarpulla, R. Young, et al., A common set of gene regulatory networks links metabolism and growth inhibition. Molecular Cell, 2004. 16(3): p. 399–411.

Figures

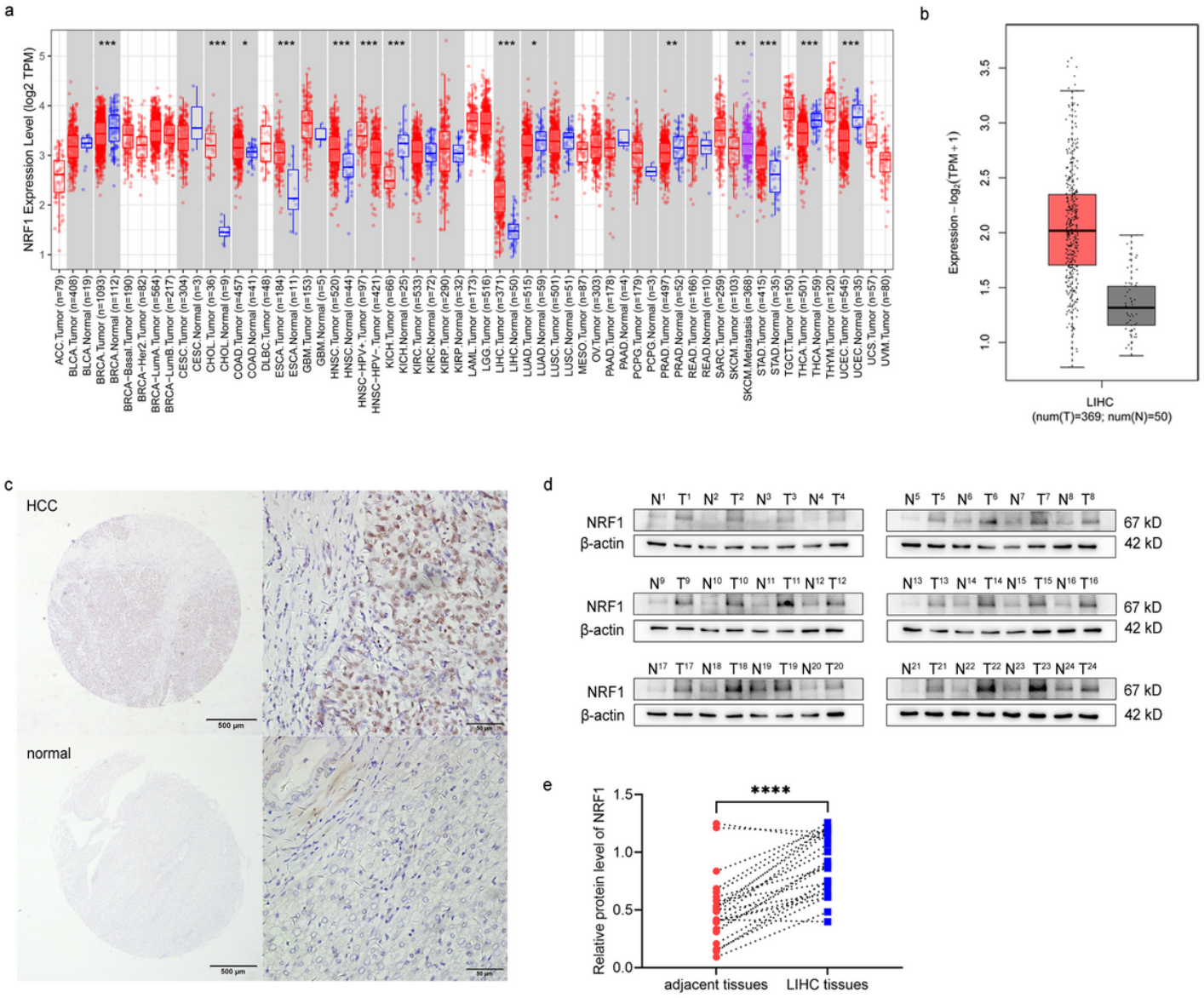

Figure 1

NRF1 expression in cancerous and normal tissues. (a) The expression of IKBIP in different human cancer tissues compared with normal tissues according to the TIMER database. (b) The level of NRF1 expression in LIHC was obtained from the GEPIA2 database. (c) Immunohistochemistry for NRF1 expression in adjacent tissue and LIHC. (d, e) NRF1 expression in 24 individual LIHC patients was analysed by Western blot and quantified using β-actin as a control. * P < 0.05, ** P < 0.01, *** P < 0.001 and **** P < 0.0001 compared with the control.

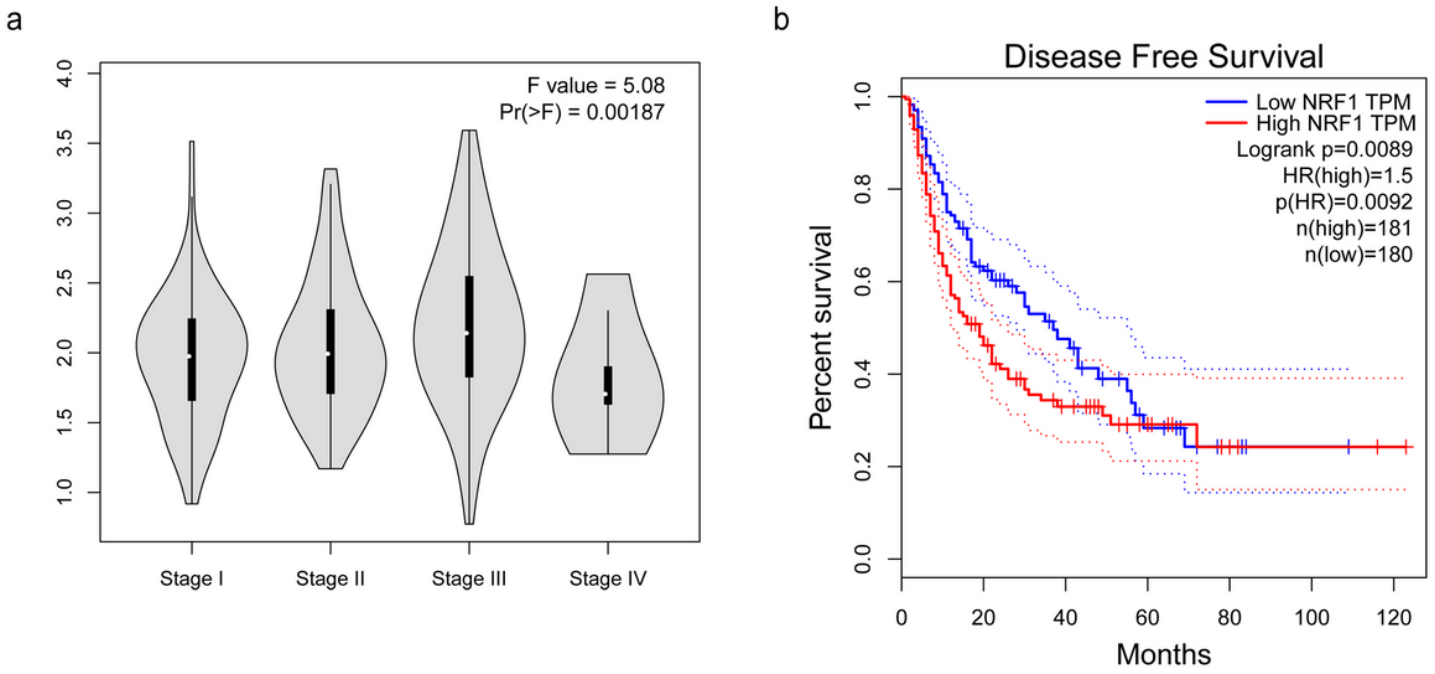

Figure 2

Association between NRF1 expression and clinicopathological parameters. (a) The association of NRF1 expression and different stages of LIHC by using GEPIA2 datasets. (b) Disease-free survival dependent on NRF1 in LIHC patients calculated by the Kaplan–Meier method. Red lines represent patients with higher expression levels of NRF1, and blue lines represent patients with lower expression levels of NRF1 (P < 0.001, log-rank test).

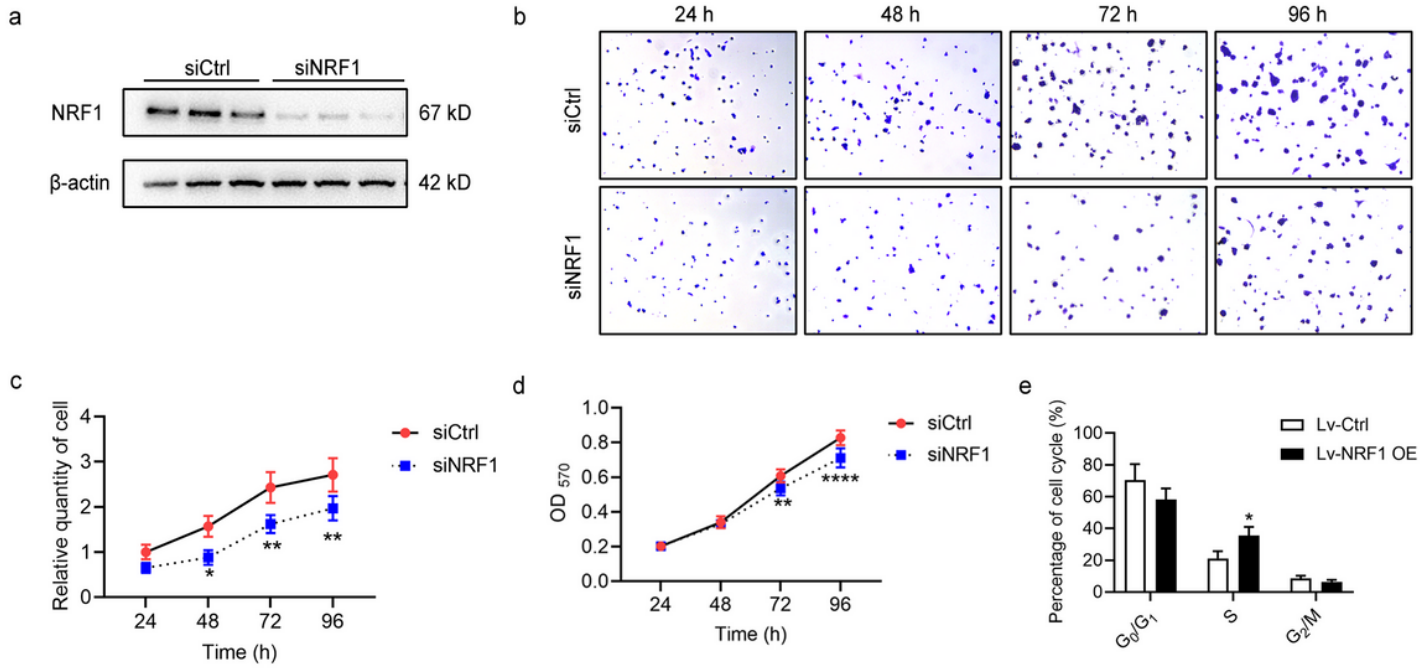

Figure 3

Effect of NRF1 on cell proliferation. (a) HepG2 cells were transfected with siCtrl or siNRF1. NRF1 and β-actin were analysed by Western blot. (b, c) Plate colony formation assays and (d) MTT assays were used to measure the impact of NRF1 knockdown on cell clonality and proliferation. (e) The cell cycle distribution of HepG2 cells with stable NRF1 expression was analysed by flow cytometry. * P < 0.05, ** P < 0.01 and **** P < 0.0001 compared with the control.

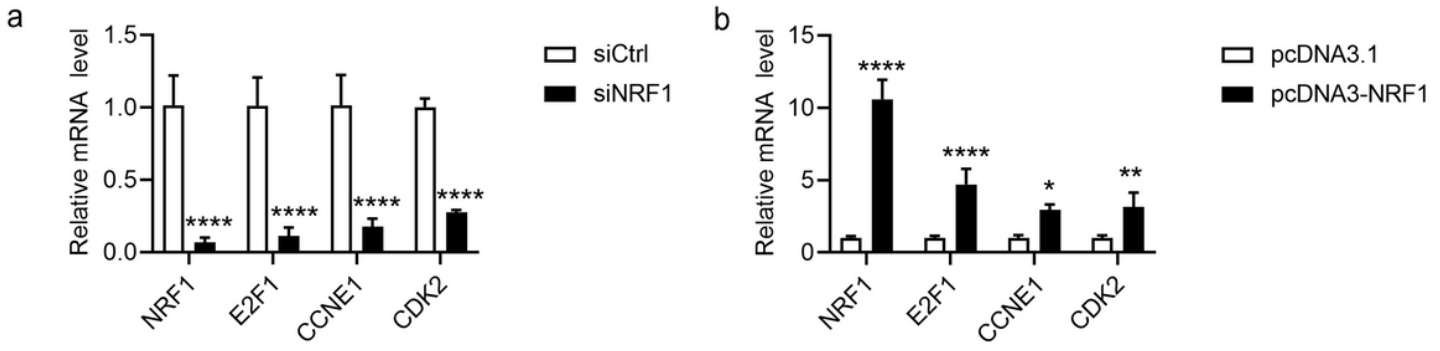

Figure 4

The effect of NRF-1 on E2F1 mRNA. HepG2 cells were transfected with siNRF1 (a) or pcDNA3-NRF1 (b). The mRNA and protein levels of NRF1, E2F1, CCNE1 and CDK2 were detected by real-time PCR and Western blot using β-actin as a control (n = 3). The data represent means ± SD. * P < 0.05, ** P < 0.01 and **** P < 0.0001 compared with the control.

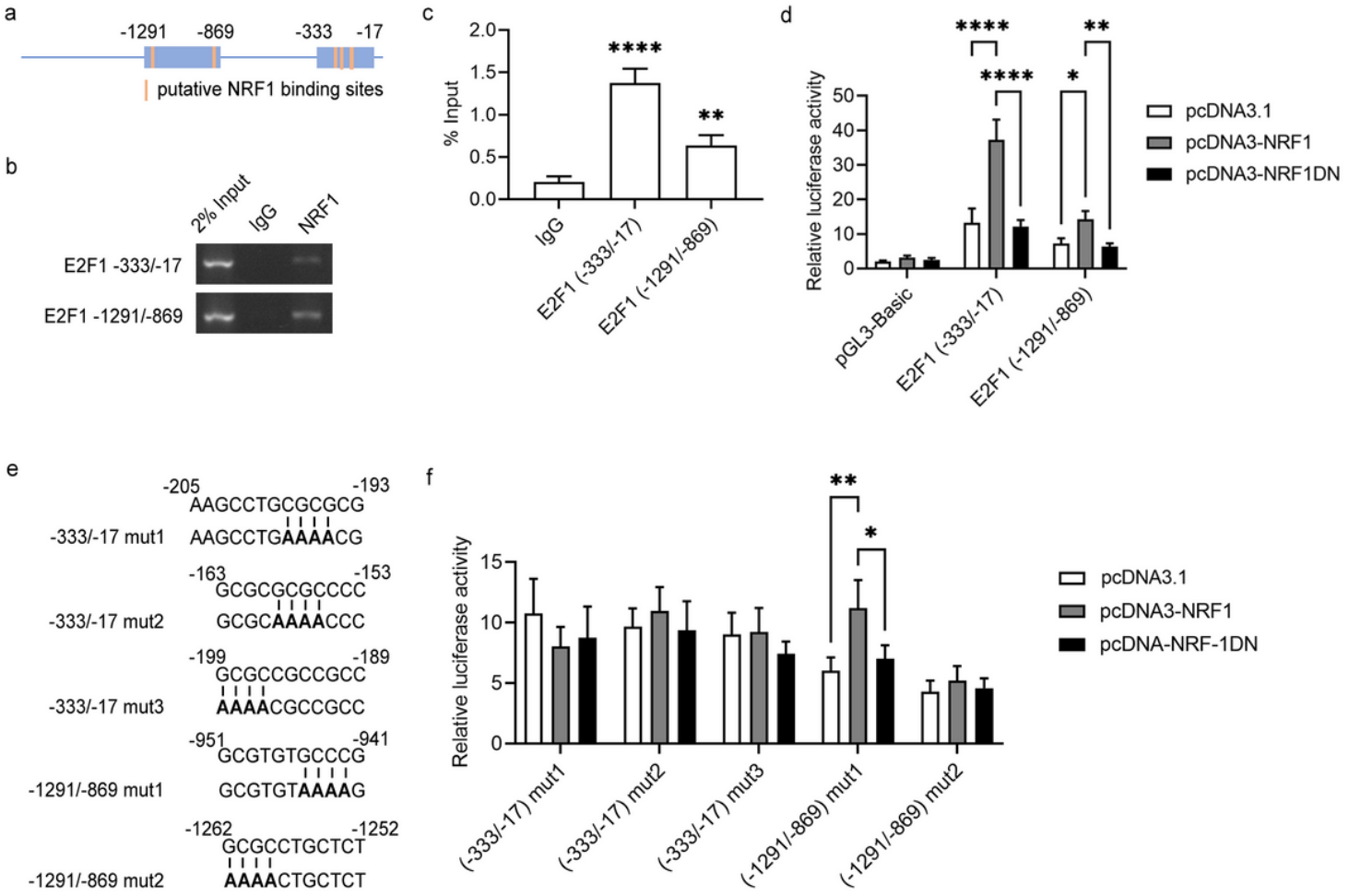

Figure 5

Identification of NRF1 binding sites in the E2F1 promoter. (a) Schematic presentation of putative NRF1 binding sites on the E2F1 promoter. (b, c) Anti-NRF1 antibody was used for the ChIP assay. Quantification of immunoprecipitated DNA fragments was performed by PCR. (d) The E2F1 constructs (-333/-17) or (-1291/-869) were cotransfected with pcDNA3-NRF1 or NRF1DN in HepG2 cells. (e) Various E2F1 (-333/-17) and (-1291/-869) constructs harbouring point mutations (mut1 to mut3) were generated and cotransfected with pcDNA3-NRF1 or NRF1DN. The pRL-TK vector was also cotransfected to normalize transfection efficiencies. The luciferase activity was determined by a dual luciferase assay. The results are presented as a luciferase/Renilla ratio. The data represent means ± SD. * $P < 0.05$, ** $P < 0.01$ and **** $P < 0.0001$ compared with the control.

Supplementary Files

This is a list of supplementary files associated with this preprint. Click to download.

- Supplements.pdf